

Observation and Properties of $L = 1$ B_1 and B_2^* Mesons

V.M. Abazov³⁵, B. Abbott⁷⁵, M. Abolins⁶⁵, B.S. Acharya²⁸, M. Adams⁵¹, T. Adams⁴⁹, E. Aguilo⁵, S.H. Ahn³⁰, M. Ahsan⁵⁹, G.D. Alexeev³⁵, G. Alkhazov³⁹, A. Alton,^{64,*} G. Alverson⁶³, G.A. Alves², M. Anastasoie³⁴, L.S. Ancu³⁴, T. Andeen⁵³, S. Anderson⁴⁵, B. Andrieu¹⁶, M.S. Anzelc⁵³, Y. Arnoud¹³, M. Arov⁶⁰, M. Arthaud¹⁷, A. Askew⁴⁹, B. Åsman,⁴⁰ A.C.S. Assis Jesus,³ O. Atramentov⁴⁹, C. Autermann²⁰, C. Avila⁷, C. Ay²³, F. Badaud¹², A. Baden⁶¹, L. Bagby⁵², B. Baldin⁵⁰, D.V. Bandurin⁵⁹, S. Banerjee²⁸, P. Banerjee²⁸, E. Barberis⁶³, A.-F. Barfuss¹⁴, P. Bargassa⁸⁰, P. Baringer⁵⁸, J. Barreto², J.F. Bartlett⁵⁰, U. Bassler¹⁶, D. Bauer⁴³, S. Beale⁵, A. Bean⁵⁸, M. Begalli³, M. Begel⁷¹, C. Belanger-Champagne⁴⁰, L. Bellantoni⁵⁰, A. Bellavance⁵⁰, J.A. Benitez⁶⁵, S.B. Beri²⁶, G. Bernardi¹⁶, R. Bernhard²², L. Berntzon¹⁴, I. Bertram⁴², M. Besançon,¹⁷ R. Beuselinck⁴³, V.A. Bezzubov³⁸, P.C. Bhat⁵⁰, V. Bhatnagar²⁶, C. Biscarat¹⁹, G. Blazey⁵², F. Blekman⁴³, S. Blessing⁴⁹, D. Bloch¹⁸, K. Bloom⁶⁷, A. Boehnlein⁵⁰, D. Boline⁶², T.A. Bolton⁵⁹, G. Borissov⁴², K. Bos³³, T. Bose⁷⁷, A. Brandt⁷⁸, R. Brock⁶⁵, G. Brooijmans⁷⁰, A. Bross⁵⁰, D. Brown⁷⁸, N.J. Buchanan⁴⁹, D. Buchholz⁵³, M. Buehler⁸¹, V. Buescher²¹, S. Burdin,^{42,¶} S. Burke⁴⁵, T.H. Burnett⁸², C.P. Buszello⁴³, J.M. Butler⁶², P. Calfayan²⁴, S. Calvet¹⁴, J. Cammin⁷¹, S. Caron³³, W. Carvalho³, B.C.K. Casey⁷⁷, N.M. Cason⁵⁵, H. Castilla-Valdez³², S. Chakrabarti¹⁷, D. Chakraborty⁵², K.M. Chan⁵⁵, K. Chan⁵, A. Chandra⁴⁸, F. Charles¹⁸, E. Cheu⁴⁵, F. Chevallier¹³, D.K. Cho⁶², S. Choi³¹, B. Choudhary²⁷, L. Christofek⁷⁷, T. Christoudias⁴³, S. Cihangir⁵⁰, D. Claes⁶⁷, C. Clément,⁴⁰ B. Clément,¹⁸ Y. Coadou⁵, M. Cooke⁸⁰, W.E. Cooper⁵⁰, M. Corcoran⁸⁰, F. Couderc¹⁷, M.-C. Cousinou¹⁴, S. Crépe-Renaudin,¹³ D. Cutts⁷⁷, M. Ćwiok,²⁹ H. da Motta,² A. Das⁶², G. Davies⁴³, K. De⁷⁸, S.J. de Jong,³⁴ P. de Jong,³³ E. De La Cruz-Burelo,⁶⁴ C. De Oliveira Martins,³ J.D. Degenhardt⁶⁴, F. Déliot,¹⁷ M. Demarteau⁵⁰, R. Demina⁷¹, D. Denisov⁵⁰, S.P. Denisov³⁸, S. Desai⁵⁰, H.T. Diehl⁵⁰, M. Diesburg⁵⁰, A. Dominguez⁶⁷, H. Dong⁷², L.V. Dudko³⁷, L. Duflot¹⁵, S.R. Dugad²⁸, D. Duggan⁴⁹, A. Duperrin¹⁴, J. Dyer⁶⁵, A. Dyshkant⁵², M. Eads⁶⁷, D. Edmunds⁶⁵, J. Ellison⁴⁸, V.D. Elvira⁵⁰, Y. Enari⁷⁷, S. Eno⁶¹, P. Ermolov³⁷, H. Evans⁵⁴, A. Evdokimov⁷³, V.N. Evdokimov³⁸, A.V. Ferapontov⁵⁹, T. Ferbel⁷¹, F. Fiedler²⁴, F. Filthaut³⁴, W. Fisher⁵⁰, H.E. Fisk⁵⁰, M. Ford⁴⁴, M. Fortner⁵², H. Fox²², S. Fu⁵⁰, S. Fuess⁵⁰, T. Gadfort⁸², C.F. Galea³⁴, E. Gallas⁵⁰, E. Galyaev⁵⁵, C. Garcia⁷¹, A. Garcia-Bellido⁸², V. Gavrilov³⁶, P. Gay¹², W. Geist¹⁸, D. Gelé,¹⁸ C.E. Gerber⁵¹, Y. Gershtein⁴⁹, D. Gillberg⁵, G. Ginter⁷¹, N. Gollub⁴⁰, B. Gómez,⁷ A. Goussiou⁵⁵, P.D. Grannis⁷², H. Greenlee⁵⁰, Z.D. Greenwood⁶⁰, E.M. Gregores⁴, G. Grenier¹⁹, Ph. Gris¹², J.-F. Grivaz¹⁵, A. Grohsjean²⁴, S. Grünendahl,⁵⁰ M.W. Grünwald,²⁹ J. Guo⁷², F. Guo⁷², P. Gutierrez⁷⁵, G. Gutierrez⁵⁰, A. Haas⁷⁰, N.J. Hadley⁶¹, P. Haefner²⁴, S. Hagopian⁴⁹, J. Haley⁶⁸, I. Hall⁷⁵, R.E. Hall⁴⁷, L. Han⁶, K. Hanagaki⁵⁰, P. Hansson⁴⁰, K. Harder⁴⁴, A. Harel⁷¹, R. Harrington⁶³, J.M. Hauptman⁵⁷, R. Hauser⁶⁵, J. Hays⁴³, T. Hebbeker²⁰, D. Hedin⁵², J.G. Hegeman³³, J.M. Heinmiller⁵¹, A.P. Heinson⁴⁸, U. Heintz⁶², C. Hensel⁵⁸, K. Herner⁷², G. Hesketh⁶³, M.D. Hildreth⁵⁵, R. Hirosky⁸¹, J.D. Hobbs⁷², B. Hoeneisen¹¹, H. Hoeth²⁵, M. Hohlfield²¹, S.J. Hong³⁰, R. Hooper⁷⁷, S. Hossain⁷⁵, P. Houben³³, Y. Hu⁷², Z. Hubacek⁹, V. Hynek⁸, I. Iashvili⁶⁹, R. Illingworth⁵⁰, A.S. Ito⁵⁰, S. Jabeen⁶², M. Jaffré,¹⁵ S. Jain⁷⁵, K. Jakobs²², C. Jarvis⁶¹, R. Jesik⁴³, K. Johns⁴⁵, C. Johnson⁷⁰, M. Johnson⁵⁰, A. Jonckheere⁵⁰, P. Jonsson⁴³, A. Juste⁵⁰, D. Käfer,²⁰ S. Kahn⁷³, E. Kajfasz¹⁴, A.M. Kalinin³⁵, J.R. Kalk⁶⁵, J.M. Kalk⁶⁰, S. Kappler²⁰, D. Karmanov³⁷, J. Kasper⁶², P. Kasper⁵⁰, I. Katsanos⁷⁰, D. Kau⁴⁹, R. Kaur²⁶, V. Kaushik⁷⁸, R. Kehoe⁷⁹, S. Kermiche¹⁴, N. Khalatyan³⁸, A. Khanov⁷⁶, A. Kharchilava⁶⁹, Y.M. Kharzheev³⁵, D. Khatidze⁷⁰, H. Kim³¹, T.J. Kim³⁰, M.H. Kirby³⁴, M. Kirsch²⁰, B. Klima⁵⁰, J.M. Kohli²⁶, J.-P. Konrath²², M. Kopal⁷⁵, V.M. Korablev³⁸, B. Kothari⁷⁰, A.V. Kozelov³⁸, D. Krop⁵⁴, A. Kryemadhi⁸¹, T. Kuhl²³, A. Kumar⁶⁹, S. Kunori⁶¹, A. Kupco¹⁰, T. Kurča,¹⁹ J. Kvita⁸, F. Lacroix¹², D. Lam⁵⁵, S. Lammers⁷⁰, G. Landsberg⁷⁷, J. Lazoflores⁴⁹, P. Lebrun¹⁹, W.M. Lee⁵⁰, A. Leflat³⁷, F. Lehner⁴¹, J. Lellouch¹⁶, V. Lesne¹², J. Leveque⁴⁵, P. Lewis⁴³, J. Li⁷⁸, Q.Z. Li⁵⁰, L. Li⁴⁸, S.M. Lietti⁴, J.G.R. Lima⁵², D. Lincoln⁵⁰, J. Linnemann⁶⁵, V.V. Lipaev³⁸, R. Lipton⁵⁰, Y. Liu⁶, Z. Liu⁵, L. Lobo⁴³, A. Lobodenko³⁹, M. Lokajicek¹⁰, A. Lounis¹⁸, P. Love⁴², H.J. Lubatti⁸², A.L. Lyon⁵⁰, A.K.A. Maciel², D. Mackin⁸⁰, R.J. Madaras⁴⁶, P. Mättig,²⁵ C. Magass²⁰, A. Magerkurth⁶⁴, N. Makovec¹⁵, P.K. Mal⁵⁵, H.B. Malbouisson³, S. Malik⁶⁷, V.L. Malyshev³⁵, H.S. Mao⁵⁰, Y. Maravin⁵⁹, B. Martin¹³, R. McCarthy⁷², A. Melnitchouk⁶⁶, A. Mendes¹⁴, L. Mendoza⁷, P.G. Mercadante⁴, M. Merkin³⁷, K.W. Merritt⁵⁰, J. Meyer²¹, A. Meyer²⁰, M. Michaut¹⁷, T. Millet¹⁹, J. Mitrevski⁷⁰, J. Molina³, R.K. Mommsen⁴⁴, N.K. Mondal²⁸, R.W. Moore⁵, T. Moulik⁵⁸, G.S. Muanza¹⁹, M. Mulders⁵⁰, M. Mulhearn⁷⁰, O. Mundal²¹, L. Mundim³, E. Nagy¹⁴, M. Naimuddin⁵⁰, M. Narain⁷⁷, N.A. Naumann³⁴, H.A. Neal⁶⁴, J.P. Negret⁷, P. Neustroev³⁹, H. Nilsen²², A. Nomerotski⁵⁰,

S.F. Novaes⁴, T. Nunnemann²⁴, V. O'Dell⁵⁰, D.C. O'Neil⁵, G. Obrant³⁹, C. Ochando¹⁵, D. Onoprienko⁵⁹,
 N. Oshima⁵⁰, J. Osta⁵⁵, R. Otec⁹, G.J. Otero y Garzón⁵¹, M. Owen⁴⁴, P. Padley⁸⁰, M. Pangilinan⁷⁷,
 N. Parashar⁵⁶, S.-J. Park⁷¹, S.K. Park³⁰, J. Parsons⁷⁰, R. Partridge⁷⁷, N. Parua⁵⁴, A. Patwa⁷³, G. Pawloski⁸⁰,
 B. Penning²², P.M. Perea⁴⁸, K. Peters⁴⁴, Y. Peters²⁵, P. Pétrouff¹⁵, M. Petteni⁴³, R. Piegaia¹, J. Piper⁶⁵,
 M.-A. Pleier²¹, P.L.M. Podesta-Lerma^{32,8}, V.M. Podstavkov⁵⁰, Y. Pogorelov⁵⁵, M.-E. Pol², P. Polozov³⁶,
 A. Pompo⁷, B.G. Pope⁶⁵, A.V. Popov³⁸, C. Potter⁵, W.L. Prado da Silva³, H.B. Prosper⁴⁹, S. Protopopescu⁷³,
 J. Qian⁶⁴, A. Quadt²¹, B. Quinn⁶⁶, A. Rakitine⁴², M.S. Rangel², K.J. Rani²⁸, K. Ranjan²⁷, P.N. Ratoff⁴²,
 P. Renkel⁷⁹, S. Reucroft⁶³, P. Rich⁴⁴, M. Rijssenbeek⁷², I. Ripp-Baudot¹⁸, F. Rizatdinova⁷⁶, S. Robinson⁴³,
 R.F. Rodrigues³, C. Royon¹⁷, P. Rubinov⁵⁰, R. Ruchti⁵⁵, G. Safronov³⁶, G. Sajot¹³, A. Sánchez-Hernández³²,
 M.P. Sanders¹⁶, A. Santoro³, G. Savage⁵⁰, L. Sawyer⁶⁰, T. Scanlon⁴³, D. Schaile²⁴, R.D. Schamberger⁷²,
 Y. Scheglov³⁹, H. Schellman⁵³, P. Schieferdecker²⁴, T. Schliephake²⁵, C. Schmitt²⁵, C. Schwanenberger⁴⁴,
 A. Schwartzman⁶⁸, R. Schwienhorst⁶⁵, J. Sekaric⁴⁹, S. Sengupta⁴⁹, H. Severini⁷⁵, E. Shabalina⁵¹, M. Shamim⁵⁹,
 V. Shary¹⁷, A.A. Shchukin³⁸, R.K. Shivpuri²⁷, D. Shpakov⁵⁰, V. Siccari¹⁸, V. Simak⁹, V. Sirotenko⁵⁰, P. Skubic⁷⁵,
 P. Slattery⁷¹, D. Smirnov⁵⁵, R.P. Smith⁵⁰, J. Snow⁷⁴, G.R. Snow⁶⁷, S. Snyder⁷³, S. Söldner-Rembold⁴⁴,
 L. Sonnenschein¹⁶, A. Sopczak⁴², M. Sosebee⁷⁸, K. Soustruznik⁸, M. Souza², B. Spurlock⁷⁸, J. Stark¹³, J. Steele⁶⁰,
 V. Stolin³⁶, A. Stone⁵¹, D.A. Stoyanova³⁸, J. Strandberg⁶⁴, S. Strandberg⁴⁰, M.A. Strang⁶⁹, M. Strauss⁷⁵,
 E. Strauss⁷², R. Ströhmer²⁴, D. Strom⁵³, M. Strovink⁴⁶, L. Stutte⁵⁰, S. Sumowidagdo⁴⁹, P. Svoisky⁵⁵,
 A. Sznajder³, M. Talby¹⁴, P. Tamburello⁴⁵, A. Tanasijczuk¹, W. Taylor⁵, P. Telford⁴⁴, J. Temple⁴⁵,
 B. Tiller²⁴, F. Tissandier¹², M. Titov¹⁷, V.V. Tokmenin³⁵, M. Tomoto⁵⁰, T. Toole⁶¹, I. Torchiani²²,
 T. Trefzger²³, D. Tsybychev⁷², B. Tuchming¹⁷, C. Tully⁶⁸, P.M. Tuts⁷⁰, R. Unalan⁶⁵, S. Uvarov³⁹, L. Uvarov³⁹,
 S. Uzunyan⁵², B. Vachon⁵, P.J. van den Berg³³, B. van Eijk³³, R. Van Kooten⁵⁴, W.M. van Leeuwen³³,
 N. Varelas⁵¹, E.W. Varnes⁴⁵, A. Vartapetian⁷⁸, I.A. Vasilyev³⁸, M. Vaupel²⁵, P. Verdier¹⁹, L.S. Vertogradov³⁵,
 M. Verzocchi⁵⁰, F. Villeneuve-Segui⁴³, P. Vint⁴³, P. Vokac⁹, E. Von Toerne⁵⁹, M. Voutilainen^{67,†},
 M. Vreeswijk³³, R. Wagner⁶⁸, H.D. Wahl⁴⁹, L. Wang⁶¹, M.H.L.S. Wang⁵⁰, J. Warchol⁵⁵, G. Watts⁸², M. Wayne⁵⁵,
 M. Weber⁵⁰, G. Weber²³, H. Weerts⁶⁵, A. Wenger^{22,‡}, N. Wermes²¹, M. Wetstein⁶¹, A. White⁷⁸, D. Wicke²⁵,
 G.W. Wilson⁵⁸, M.R.J. Williams⁴², S.J. Wimpenny⁴⁸, M. Wobisch⁶⁰, D.R. Wood⁶³, T.R. Wyatt⁴⁴,
 Y. Xie⁷⁷, S. Yacoub⁵³, R. Yamada⁵⁰, M. Yan⁶¹, T. Yasuda⁵⁰, Y.A. Yatsunenko³⁵, K. Yip⁷³, H.D. Yoo⁷⁷,
 S.W. Youn⁵³, J. Yu⁷⁸, C. Yu¹³, A. Yurkewicz⁷², A. Zatserklyaniy⁵², C. Zeitnitz²⁵, D. Zhang⁵⁰, T. Zhao⁸²,
 B. Zhou⁶⁴, J. Zhu⁷², M. Zielinski⁷¹, D. Zieminska⁵⁴, A. Zieminski⁵⁴, L. Zivkovic⁷⁰, V. Zutshi⁵², and E.G. Zverev³⁷

(The DØ Collaboration)

¹ Universidad de Buenos Aires, Buenos Aires, Argentina

² LAFEX, Centro Brasileiro de Pesquisas Físicas, Rio de Janeiro, Brazil

³ Universidade do Estado do Rio de Janeiro, Rio de Janeiro, Brazil

⁴ Instituto de Física Teórica, Universidade Estadual Paulista, São Paulo, Brazil

⁵ University of Alberta, Edmonton, Alberta, Canada,
 Simon Fraser University, Burnaby, British Columbia,
 Canada, York University, Toronto, Ontario, Canada,
 and McGill University, Montreal, Quebec, Canada

⁶ University of Science and Technology of China, Hefei, People's Republic of China

⁷ Universidad de los Andes, Bogotá, Colombia

⁸ Center for Particle Physics, Charles University, Prague, Czech Republic

⁹ Czech Technical University, Prague, Czech Republic

¹⁰ Center for Particle Physics, Institute of Physics,
 Academy of Sciences of the Czech Republic, Prague, Czech Republic

¹¹ Universidad San Francisco de Quito, Quito, Ecuador

¹² Laboratoire de Physique Corpusculaire, IN2P3-CNRS,
 Université Blaise Pascal, Clermont-Ferrand, France

¹³ Laboratoire de Physique Subatomique et de Cosmologie,
 IN2P3-CNRS, Université de Grenoble 1, Grenoble, France

¹⁴ CPPM, IN2P3-CNRS, Université de la Méditerranée, Marseille, France

¹⁵ Laboratoire de l'Accélérateur Linéaire, IN2P3-CNRS et Université Paris-Sud, Orsay, France

¹⁶ LPNHE, IN2P3-CNRS, Universités Paris VI and VII, Paris, France

¹⁷ DAPNIA/Service de Physique des Particules, CEA, Saclay, France

¹⁸ IPHC, Université Louis Pasteur et Université de Haute Alsace, CNRS, IN2P3, Strasbourg, France

¹⁹ IPNL, Université Lyon 1, CNRS/IN2P3, Villeurbanne, France and Université de Lyon, Lyon, France

²⁰ III. Physikalisches Institut A, RWTH Aachen, Aachen, Germany

- ²¹Physikalisches Institut, Universität Bonn, Bonn, Germany
- ²²Physikalisches Institut, Universität Freiburg, Freiburg, Germany
- ²³Institut für Physik, Universität Mainz, Mainz, Germany
- ²⁴Ludwig-Maximilians-Universität München, München, Germany
- ²⁵Fachbereich Physik, University of Wuppertal, Wuppertal, Germany
- ²⁶Panjab University, Chandigarh, India
- ²⁷Delhi University, Delhi, India
- ²⁸Tata Institute of Fundamental Research, Mumbai, India
- ²⁹University College Dublin, Dublin, Ireland
- ³⁰Korea Detector Laboratory, Korea University, Seoul, Korea
- ³¹SungKyunKwan University, Suwon, Korea
- ³²CINVESTAV, Mexico City, Mexico
- ³³FOM-Institute NIKHEF and University of Amsterdam/NIKHEF, Amsterdam, The Netherlands
- ³⁴Radboud University Nijmegen/NIKHEF, Nijmegen, The Netherlands
- ³⁵Joint Institute for Nuclear Research, Dubna, Russia
- ³⁶Institute for Theoretical and Experimental Physics, Moscow, Russia
- ³⁷Moscow State University, Moscow, Russia
- ³⁸Institute for High Energy Physics, Protvino, Russia
- ³⁹Petersburg Nuclear Physics Institute, St. Petersburg, Russia
- ⁴⁰Lund University, Lund, Sweden, Royal Institute of Technology and Stockholm University, Stockholm, Sweden, and Uppsala University, Uppsala, Sweden
- ⁴¹Physik Institut der Universität Zürich, Zürich, Switzerland
- ⁴²Lancaster University, Lancaster, United Kingdom
- ⁴³Imperial College, London, United Kingdom
- ⁴⁴University of Manchester, Manchester, United Kingdom
- ⁴⁵University of Arizona, Tucson, Arizona 85721, USA
- ⁴⁶Lawrence Berkeley National Laboratory and University of California, Berkeley, California 94720, USA
- ⁴⁷California State University, Fresno, California 93740, USA
- ⁴⁸University of California, Riverside, California 92521, USA
- ⁴⁹Florida State University, Tallahassee, Florida 32306, USA
- ⁵⁰Fermi National Accelerator Laboratory, Batavia, Illinois 60510, USA
- ⁵¹University of Illinois at Chicago, Chicago, Illinois 60607, USA
- ⁵²Northern Illinois University, DeKalb, Illinois 60115, USA
- ⁵³Northwestern University, Evanston, Illinois 60208, USA
- ⁵⁴Indiana University, Bloomington, Indiana 47405, USA
- ⁵⁵University of Notre Dame, Notre Dame, Indiana 46556, USA
- ⁵⁶Purdue University Calumet, Hammond, Indiana 46323, USA
- ⁵⁷Iowa State University, Ames, Iowa 50011, USA
- ⁵⁸University of Kansas, Lawrence, Kansas 66045, USA
- ⁵⁹Kansas State University, Manhattan, Kansas 66506, USA
- ⁶⁰Louisiana Tech University, Ruston, Louisiana 71272, USA
- ⁶¹University of Maryland, College Park, Maryland 20742, USA
- ⁶²Boston University, Boston, Massachusetts 02215, USA
- ⁶³Northeastern University, Boston, Massachusetts 02115, USA
- ⁶⁴University of Michigan, Ann Arbor, Michigan 48109, USA
- ⁶⁵Michigan State University, East Lansing, Michigan 48824, USA
- ⁶⁶University of Mississippi, University, Mississippi 38677, USA
- ⁶⁷University of Nebraska, Lincoln, Nebraska 68588, USA
- ⁶⁸Princeton University, Princeton, New Jersey 08544, USA
- ⁶⁹State University of New York, Buffalo, New York 14260, USA
- ⁷⁰Columbia University, New York, New York 10027, USA
- ⁷¹University of Rochester, Rochester, New York 14627, USA
- ⁷²State University of New York, Stony Brook, New York 11794, USA
- ⁷³Brookhaven National Laboratory, Upton, New York 11973, USA
- ⁷⁴Langston University, Langston, Oklahoma 73050, USA
- ⁷⁵University of Oklahoma, Norman, Oklahoma 73019, USA
- ⁷⁶Oklahoma State University, Stillwater, Oklahoma 74078, USA
- ⁷⁷Brown University, Providence, Rhode Island 02912, USA
- ⁷⁸University of Texas, Arlington, Texas 76019, USA
- ⁷⁹Southern Methodist University, Dallas, Texas 75275, USA
- ⁸⁰Rice University, Houston, Texas 77005, USA
- ⁸¹University of Virginia, Charlottesville, Virginia 22901, USA and
- ⁸²University of Washington, Seattle, Washington 98195, USA

(Dated: May 22, 2007)

Excited B mesons B_1 and B_2^* are observed directly for the first time as two separate states in fully reconstructed decays to $B^{(*)}\pi^-$. The mass of B_1 is measured to be $5720.6 \pm 2.4 \pm 1.4$ MeV/ c^2 and the mass difference ΔM between B_2^* and B_1 is $26.2 \pm 3.1 \pm 0.9$ MeV/ c^2 , giving the mass of the B_2^* as $5746.8 \pm 2.4 \pm 1.7$ MeV/ c^2 . The production rate for B_1 and B_2^* mesons is determined to be a fraction $(13.9 \pm 1.9 \pm 3.2)\%$ of the production rate of the B^+ meson.

PACS numbers: 12.15.Ff, 13.20.He, 14.40.Nd

To date, the detailed spectroscopy of mesons containing a b quark has not been fully established. Only the ground 0^- states B^+ , B^0 , B_s^0 , B_c^+ and the excited 1^- state B^* are considered to be established by the PDG [1]. Quark models predict the existence of two broad (B_0^* [$J^P = 0^+$] and B_1^* [1^+]) and two narrow (B_1 [1^+] and B_2^* [2^+]) bound P states [2–7]. The broad states decay through an S wave and therefore have widths of a few hundred MeV/ c^2 . Such states are difficult to distinguish, in effective mass spectra, from the combinatorial background. The narrow states decay through a D wave and therefore should have widths of around 10 MeV/ c^2 [3, 6, 7]. Almost all observations of B_1 and B_2^* have been made indirectly in inclusive or semi-inclusive decays [8–11], which prevents their separation and a precise measurement of their properties. The measurement by the ALEPH collaboration [12], although partially done with exclusive B decays, was statistically limited and model dependent. The masses, widths, and decay branching fractions of these states, in contrast, are predicted with good precision by various theoretical models [2–7]. These predictions can be verified experimentally, and such a comparison provides important information on the quark interaction inside bound states, aiding further development of non-perturbative QCD. This Letter presents a study of narrow $L = 1$ states decaying to $B^{(*)}\pi^-$ with exclusively reconstructed B^+ mesons using data collected by the D0 experiment during 2002–2006 and corresponding to an integrated luminosity of about 1.3 fb^{-1} . Throughout this Letter, charge conjugated states are implied.

The D0 detector is described in detail elsewhere [13]. The detector components most important for this analysis are the central tracking and muon systems. The D0 central tracking system consists of a silicon microstrip tracker (SMT) and a central fiber tracker (CFT), both located within a 2 T superconducting solenoidal magnet, with designs optimized for tracking and vertexing at pseudorapidities $|\eta| < 3$ and $|\eta| < 2.5$, respectively (where $\eta = -\ln[\tan(\theta/2)]$, and θ is the polar angle measured with respect to the beam line). The muon system is located outside the calorimeters and has pseudorapidity coverage $|\eta| < 2$. It consists of a layer of tracking detectors and scintillation trigger counters in front of 1.8 T toroids, followed by two similar layers behind the toroids [14].

The B_1 and B_2^* mesons are studied by examining $B^{(*)}\pi^-$ candidates. This sample includes the following

decays:

$$B_1 \rightarrow B^{*+}\pi^-; B^{*+} \rightarrow B^+\gamma; \quad (1)$$

$$B_2^* \rightarrow B^{*+}\pi^-; B^{*+} \rightarrow B^+\gamma; \quad (2)$$

$$B_2^* \rightarrow B^+\pi^-. \quad (3)$$

The direct decay $B_1 \rightarrow B^+\pi^-$ is forbidden by conservation of parity and angular momentum. The B^+ meson is reconstructed in the exclusive decay $B^+ \rightarrow J/\psi K^+$ with J/ψ decaying to $\mu^+\mu^-$. Each muon is required to be identified by the muon system, have an associated track in the central tracking system with at least two measurements in the SMT, and a transverse momentum $p_T^\mu > 1.5$ GeV/ c . At least one of the two muons is required to have matching track segments both inside and outside the toroidal magnet. The two muons must form a common vertex and have an invariant mass between 2.80 and 3.35 GeV/ c^2 , to form a J/ψ candidate. An additional charged track with $p_T > 0.5$ GeV/ c , with total momentum above 0.7 GeV/ c and with at least two measurements in the SMT, is selected. This particle is assigned the kaon mass and required to have a common vertex, with $\chi^2 < 16$ for 3 degrees of freedom, with the two muons. The displacement of this vertex from the primary interaction point is required to exceed three standard deviations in the plane perpendicular to the beam direction. The primary vertex of the $p\bar{p}$ interaction was determined for each event using the method described in Ref. [15]. The average position of the beam-collision point was included as a constraint.

From each set of three particles fulfilling these requirements, a B^+ candidate is constructed. The momenta of the muons are corrected using the J/ψ mass [1] as a constraint. To further improve the B^+ selection, a likelihood ratio method [16] is utilized. This method provides a simple way of combining several discriminating variables into a single variable with increased power to separate signal and background. The variables chosen for this analysis include the smaller of the transverse momenta of the two muons, the χ^2 of the B^+ decay vertex, the B^+ decay length divided by its error, the significance (defined below) S_B of the B^+ track impact parameter, the transverse momentum of the kaon, and the significance S_K of the kaon track impact parameter.

For any track i , the significance S_i is defined as $S_i = \sqrt{[\epsilon_T/\sigma(\epsilon_T)]^2 + [\epsilon_L/\sigma(\epsilon_L)]^2}$, where ϵ_T (ϵ_L) is the projection of the track impact parameter on the plane perpendicular to the beam direction (along the beam direction), and $\sigma(\epsilon_T)$ [$\sigma(\epsilon_L)$] is its uncertainty. The track of each

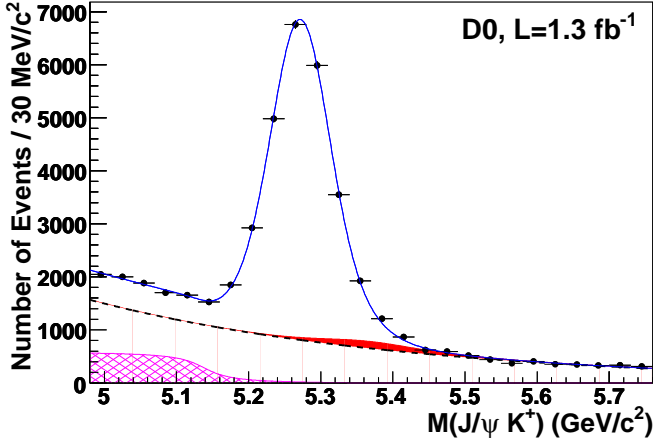


FIG. 1: Invariant mass distribution of $J/\psi K^+$ events. The solid line shows the sum of signal and background contributions, as described in the text. The contribution of $J/\psi\pi^+$ events is shown by the solid filled area and the $J/\psi K^{*+}$ contribution is shown by the hatched area. The dashed line shows the exponential function modeling the combinatorial background.

B^+ is formed assuming that it passes through the reconstructed vertex and is directed along the reconstructed B^+ momentum.

The resulting invariant mass distribution of the $J/\psi K^+$ system is shown in Fig. 1. The curve represents the result of an unbinned likelihood fit to the sum of contributions from $B^+ \rightarrow J/\psi K^+$, $B^+ \rightarrow J/\psi\pi^+$, and $B^+ \rightarrow J/\psi K^{*+}$ decays, as well as combinatorial background. The mass distribution of the $J/\psi K^+$ system from the $B^+ \rightarrow J/\psi K^+$ hypothesis is parameterized by a Gaussian with the width depending on the momentum of the K^+ . For the contribution from $B^+ \rightarrow J/\psi\pi^+$ decays, the width of the $J/\psi\pi^+$ mass distribution is parametrized with the same momentum-dependent width as the $B^+ \rightarrow J/\psi K^+$ decays, and then transformed to the $J/\psi K^+$ system by assigning the kaon mass to the charged pion. The decay $B \rightarrow J/\psi K^{*+}$ with $K^{*+} \rightarrow K\pi$ produces a broad $J/\psi K^+$ mass distribution with the threshold near $M(B) - M(\pi)$. It is parameterized using Monte Carlo simulation (described later). The combinatorial background is described by an exponential function. The $B^+ \rightarrow J/\psi K^+$ and $B^+ \rightarrow J/\psi\pi^+$ mass peaks contain 23287 ± 344 (stat.) events.

For each reconstructed B meson candidate with mass $5.19 < M(B^+) < 5.36$ GeV/c^2 , an additional charged track with transverse momentum above 0.75 GeV/c and charge opposite to that of the B meson is selected. The selection $5.19 < M(B^+) < 5.36$ GeV/c^2 reduces the number of B^+ candidates to 20915 ± 293 (stat.). Since the B_J mesons (where B_J denotes both B_1 and B_2^*) decay at the production point, the additional track is required to originate from the primary vertex by applying

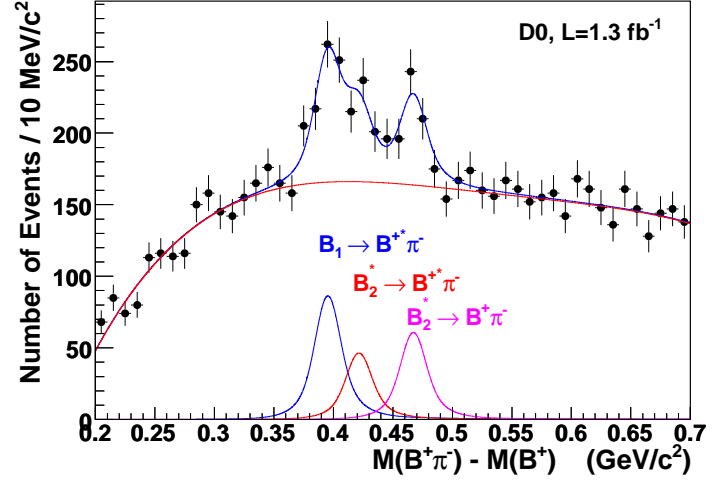


FIG. 2: Invariant mass difference $\Delta M = M(B^+\pi^-) - M(B^+)$ for exclusive B decays. The line shows the fit described in the text. The contribution of background and the three signal peaks are shown separately [color online].

the condition on its significance $S_\pi < \sqrt{6}$.

For each combination satisfying the above criteria, the mass difference $\Delta M = M(B^+\pi^-) - M(B^+)$ is computed. The resulting distribution of ΔM is shown in Fig. 2. The signal exhibits a structure that is interpreted in terms of the decays (1–3). Since the photon from the decay $B^* \rightarrow B\gamma$ is not reconstructed, the three decays should produce three peaks with central positions $\Delta_1 = M(B_1) - M(B^*)$, corresponding to the decay $B_1 \rightarrow B^*\pi$, $\Delta_2 = M(B_2^*) - M(B^*)$, corresponding to $B_2^* \rightarrow B^*\pi$, and $\Delta_3 = M(B_2^*) - M(B)$, corresponding to $B_2^* \rightarrow B\pi$. Note that in this case, $\Delta_2 = \Delta_3 - [M(B^{*+}) - M(B)] = \Delta_3 - 45.78$ MeV/c^2 [1]. Following this expected pattern, the experimental distribution is fitted to the following function:

$$\begin{aligned} F(\Delta M) &= F_{\text{sig}}(\Delta M) + F_{\text{bckg}}(\Delta M), \\ F_{\text{sig}}(\Delta M) &= N \cdot \{f_1 \cdot D(\Delta M, \Delta_1, \Gamma_1) \\ &\quad + (1 - f_1) \cdot [f_2 \cdot D(\Delta M, \Delta_2, \Gamma_2) \\ &\quad + (1 - f_2) \cdot D(\Delta M, \Delta_3, \Gamma_2)]\}. \end{aligned} \quad (4)$$

In these equations, Γ_1 and Γ_2 are the widths of B_1 and B_2^* , f_1 is the fraction of B_1 contained in the B_J signal, and f_2 is the fraction of $B_2^* \rightarrow B^*\pi$ decays in the B_2^* signal. The parameter N gives the total number of observed $B_J \rightarrow B^{+(*)}\pi$ decays. The background $F_{\text{bckg}}(\Delta M)$ is parameterized by a fourth-order polynomial.

The function $D(x, x_0, \Gamma)$ in Eq. (4) is the convolution of a relativistic Breit-Wigner function with the experimental Gaussian resolution in ΔM . The width of resonances in the Breit-Wigner function takes into account threshold effects using the standard expression:

$$\Gamma(x) = \Gamma_0 \frac{x_0}{x} \left(\frac{k}{k_0} \right)^5 F^{(2)}(k, k_0). \quad (5)$$

The variables k and k_0 in Eq. (5) are the magnitudes of the pion three-momentum in the B_J rest frame when B_J has a four-momentum-squared equal to x^2 and x_0^2 , respectively. Γ_0 is the total decay width, and $F^{(2)}(k, k_0)$ is the Blatt-Weiskopf form factor for $L = 2$ decay [1, 17].

The resolution in ΔM is determined from simulation. All processes involving B mesons are simulated using the EVTGEN generator [18] interfaced with PYTHIA [19], followed by full modeling of the detector response with GEANT [20] and event reconstruction as in data. The difference between the reconstructed and generated values of ΔM is parameterized by a double Gaussian function with the σ of the narrow Gaussian set to $7.5 \text{ MeV}/c^2$, the σ of the wide Gaussian set to $17.6 \text{ MeV}/c^2$, and the normalisation of the narrow Gaussian set to 3.8 times that of the wide Gaussian. Studies of the $B^+ \rightarrow J/\psi K^+$ mass peak show that simulation underestimates the mass resolution in data by $\approx 10\%$. As such, the widths of the Gaussians which parameterise the B_J resolution are increased by 10% to match the data, and a 100% systematic uncertainty is assigned to this correction. The widths of the observed structures are compatible with the experimental mass resolution, and the fit is found to be insensitive to values of Γ_1 and Γ_2 below the mass resolution with the current statistics. Therefore, both these widths are fixed at $10 \text{ MeV}/c^2$ in the fit, as suggested by theoretical models [3, 7]. They are varied together over a wide range to estimate the associated systematic uncertainty.

With these assumptions, the following parameters of B_1 and B_2^* are obtained:

$$\begin{aligned} M(B_1) - M(B^+) &= 441.5 \pm 2.4 \pm 1.3 \text{ MeV}/c^2, \\ M(B_2^*) - M(B_1) &= 26.2 \pm 3.1 \pm 0.9 \text{ MeV}/c^2. \end{aligned} \quad (6)$$

where the first uncertainty is statistical, and the second is systematic. The correlation coefficient of these mass measurements is -0.659 . With these relations, and using the mass of the B^+ [1], the absolute masses of the B_1 and B_2^* are:

$$\begin{aligned} M(B_1) &= 5720.6 \pm 2.4 \pm 1.4 \text{ MeV}/c^2, \\ M(B_2^*) &= 5746.8 \pm 2.4 \pm 1.7 \text{ MeV}/c^2. \end{aligned} \quad (7)$$

The number of B_J decays is found to be $N = 662 \pm 91$. The $\chi^2/\text{d.o.f.}$ of the fit is 33/40. Without the B_J signal contribution, the $\chi^2/\text{d.o.f.}$ of the fit increases to 97/45, which implies that this structure is observed with a statistical significance of more than 7σ . Fitting with only one peak increases the $\chi^2/\text{d.o.f.}$ to 54/42, which corresponds to more than a 4σ significance that more than one resonance is observed. With the $B_2^* \rightarrow B^{*+}\pi$ decay removed from the fit, the $\chi^2/\text{d.o.f.}$ of the fit increases to 41/41. Although with the current statistics we can not distinguish between the two- and three- peaks hypotheses, theory suggests that B_2^* decays with almost equal branching ratios into $B\pi$ and $B^{*+}\pi$ [3, 7], and our fit indeed indicates a preference for this expected pattern.

The number of B_J mesons and values f_1 and f_2 obtained from the fit are used to measure the production and decay ratios of B_1 and B_2^* :

$$\begin{aligned} R_1 &= \frac{Br(B_1 \rightarrow B^{*+}\pi)}{Br(B_J \rightarrow B^{(*)}\pi)} = f_1 \cdot \frac{\varepsilon_0}{\varepsilon_1} \\ &= 0.477 \pm 0.069 \pm 0.062, \\ R_2 &= \frac{Br(B_2^* \rightarrow B^{*+}\pi)}{Br(B_2^* \rightarrow B^{(*)}\pi)} = f_2 \cdot \frac{\varepsilon_3}{\varepsilon_2} \\ &= 0.475 \pm 0.095 \pm 0.069, \\ R_J &= \frac{Br(b \rightarrow B_J^0 \rightarrow B^{(*)}\pi)}{Br(b \rightarrow B^+)} = \frac{3 \cdot N(B_J)}{2 \cdot N(B^+) \cdot \varepsilon_0} \\ &= 0.139 \pm 0.019 \pm 0.032. \end{aligned} \quad (8)$$

Here ε_1 , ε_2 and ε_3 are the efficiencies to select an additional pion from the B_J decay for decay modes $B_1 \rightarrow B^{*+}\pi^-$, $B_2^* \rightarrow B^{*+}\pi^-$ and $B_2^* \rightarrow B^+\pi^-$, respectively. They are determined from a simulation separately for each decay mode (1–3). The overall efficiency for detecting a pion from any $B_J \rightarrow B^{(*)}\pi^-$ decay is $\varepsilon_0 = 0.342 \pm 0.008 \pm 0.028$. The value for R_J takes into account the decay $B_J \rightarrow B^0\pi^0$ assuming isospin conservation.

For the B_J mass fit, the influences of different sources of systematic uncertainty are estimated by examining the changes in the fit parameters under a number of variations. Different background parameterizations are used in the fit to the ΔM distribution. In addition, the effect of binning is tested by varying the bin width and position. The parameters describing the background are allowed to vary in the fit and their uncertainties are included in our results. To check the effect of fixing Γ_1 and Γ_2 at $10 \text{ MeV}/c^2$, a range of widths from 0 to $20 \text{ MeV}/c^2$ is used. The effect of the uncertainty on the mass difference $M(B^{*+}) - M(B^+)$ [1] is also taken into account. Different parameterizations of the detector mass resolution are tested, and in addition the fit is made without the 10% mass resolution correction. The uncertainty in the absolute momentum scale, which results in a small shift of all measured masses, is also taken into account. The summary of all systematic uncertainties in the B_J mass fit is given in Table I.

The measurement of the relative production rate R_J uses the pion detection efficiencies predicted in simulation, as well as the numbers of B_J and B^+ events. To estimate the systematic uncertainty on the number of B^+ events, different parameterizations of the signal and background are used for the fit. The resulting uncertainty is $\pm 200 B^+$ events. The systematic uncertainty on the number of B_J events is ± 140 (see Table I). The uncertainty of the impact parameter resolution in the simulation is estimated to be $\approx 10\%$ [22]. It can influence the measurement of the selection efficiency of the pion from the B_J decay, and its contribution to the systematic uncertainty of R_J is found to be 0.0056. The track reconstruction efficiency for particles with low transverse

TABLE I: Systematic uncertainties of the B_J parameters determined from the ΔM fit. The rows show the various sources of systematic error as described in the text. The columns show the resulting uncertainties for each of the five free signal parameters as described in Eq. (4). $\Delta M(B_1)$ and $\Delta[M(B_2^*) - M(B_1)]$ are in MeV/ c^2 .

Source	$\Delta M(B_1)$	$\Delta[M(B_2^*) - M(B_1)]$	ΔR_1	ΔR_2	ΔN
Background parameterization	0.15	0.15	0.010	0.009	19
Bin widths/positions	0.85	0.70	0.006	0.026	12
Value of Γ	0.75	0.55	0.023	0.032	138
B^{+*} mass uncertainty	0.30	0.25	0.004	0.004	6
Momentum scale	0.50	0.03	0.000	0.000	0
Resolution uncertainty	0.20	0.05	0.007	0.004	10
Efficiency uncertainties			0.056	0.054	
Total	1.30	0.90	0.062	0.069	140

momentum is measured in Ref. [21] and good agreement between data and simulation is found. This comparison is valid within the uncertainties of branching fractions of different B semileptonic decays, which is about 7%. This uncertainty results in a 0.0096 variation of R_J . An additional systematic uncertainty of 0.0008 associated with the difference in the momentum distributions of selected particles in data and in simulation is taken into account. Combining all these effects in quadrature, the total systematic uncertainty in the relative production rate R_J is found to be 0.032, of which the dominant contribution comes from the uncertainty on the number of B_J events.

Different consistency checks of the observed signal are performed. The stability of the fit under different selections of π meson from $B_J \rightarrow B^{+(*)}\pi$ decay and the width of the B^+ mass window is verified. Events with positively and negatively charged pions are analyzed separately, and consistent results are obtained. A complementary sample of events containing a pion not compatible with the primary vertex is selected, and no significant B_J signal is observed. Events with wrong charge combinations ($B^+\pi^+$ and $B^-\pi^-$) also show a signal consistent with zero. In addition, the fit is repeated without the Blatt-Weiskopf form-factor and no visible change in results is observed.

In conclusion, the B_1 and B_2^* mesons are observed for the first time as two separate states. Their measured masses are given by Eq. (6). The B_J production rate, the branching fraction of B_2^* to the excited state B^* , and the fraction of the B_1 meson in the B_J production rate are also measured as given in Eq. (8). These results will help to develop models describing bound states with heavy quarks.

We thank the staffs at Fermilab and collaborating institutions, and acknowledge support from the DOE and NSF (USA); CEA and CNRS/IN2P3 (France); FASI, Rosatom and RFBR (Russia); CAPES, CNPq, FAPERJ, FAPESP and FUNDUNESP (Brazil); DAE and DST (India); Colciencias (Colombia); CONACyT (Mexico); KRF and KOSEF (Korea); CONICET and UBACyT (Argentina); FOM (The Netherlands); PPARC (United Kingdom); MSMT (Czech Republic); CRC Program,

CFI, NSERC and WestGrid Project (Canada); BMBF and DFG (Germany); SFI (Ireland); The Swedish Research Council (Sweden); Research Corporation; Alexander von Humboldt Foundation; and the Marie Curie Program.

-
- [*] Visitor from Augustana College, Sioux Falls, SD, USA.
 - [¶] Visitor from The University of Liverpool, Liverpool, UK.
 - [§] Visitor from ICN-UNAM, Mexico City, Mexico.
 - [‡] Visitor from Helsinki Institute of Physics, Helsinki, Finland.
 - [#] Visitor from Universität Zürich, Zürich, Switzerland.
 - [1] W.-M. Yao *et al.* (Particle Data Group), J. Phys. G **33**, 1 (2006).
 - [2] T. Matsuki and T. Morii, Phys. Rev. D **56**, 5646 (1997); T. Matsuki, T. Morii and K. Sudoh, arXiv:hep-ph/0605019.
 - [3] M. Di Pierro and E. Eichten, Phys. Rev. D **64**, 114004 (2001); E.J. Eichten, C.T. Hill, C. Quigg, Phys. Rev. Lett. **71**, 4116 (1993).
 - [4] N. Isgur, Phys. Rev. D **57**, 4041 (1998).
 - [5] D. Ebert, V.O. Galkin, R.N. Faustov, Phys. Rev. D **57**, 5663 (1998), Erratum Phys. Rev. D **59**, 019902 (1999).
 - [6] A.H. Orsland, H. Hogaasen, Eur. Phys. J. **C9**, 503 (1999).
 - [7] A. Falk, T. Mehen, Phys. Rev. D **53**, 231 (1996).
 - [8] OPAL Collaboration, R. Akers *et al.*, Z. Phys. C **66**, 19 (1995).
 - [9] DELPHI Collaboration, P. Abreu *et al.*, Phys. Lett. B **345**, 598 (1995).
 - [10] ALEPH Collaboration, D. Buskulic *et al.*, Z. Phys. C **69**, 393 (1996).
 - [11] CDF Collaboration, T. Affolder *et al.*, Phys. Rev. D **64**, 072002 (2001).
 - [12] ALEPH Collaboration, R. Barate *et al.*, Phys. Lett. B **425**, 215 (1998).
 - [13] D0 Collaboration, V.M. Abazov *et al.*, Nucl. Instrum. Methods A **565**, 463 (2006).
 - [14] D0 Collaboration, V.M. Abazov *et al.*, Nucl. Instrum. Methods A **552**, 372 (2005).
 - [15] DELPHI Collaboration, J. Abdallah *et al.*, Eur. Phys. J **C32**, 185 (2004).
 - [16] G. Borisov, Nucl. Instrum. Methods A **417**, 384 (1998).

- [17] J. Blatt and V. Weisskopf, Theoretical Nuclear Physics (John Wiley & Sons, New York, 1952), p. 361.
- [18] D.J. Lange, Nucl. Instrum. Methods A **462**, 152 (2001).
- [19] T. Sjöstrand *et al.*, Comp. Phys. Commun. **135**, 238 (2001).
- [20] R. Brun and F. Carminati, CERN Program Library Long Writeup **W5013** (1993).
- [21] D0 Collaboration, V.M. Abazov *et al.*, Phys. Rev. Lett. **94**, 182001 (2005).
- [22] D0 Collaboration, V.M. Abazov *et al.*, Phys. Rev. Lett. **97**, 021802 (2006).